Total Ionizing Dose Analysis with EDGE/SSAM of 1U and 6U CubeSats in Realistic Proton and Electron Environments

B. Tezenas du Montcel[1,*], B. Jeanty-Ruard[1], J. Forest[2], A. Trouche[1], N. Chabalier[1]

[1]*Artenum*, Toulouse, France
[2]*Artenum*, Paris, France
[*]tezenas-du-montcel@artenum.com

***Abstract*—The Sector Shielding Analysis Module (SSAM), a plug-in for the ExtendeD Gdml Editor, which employs a ray-tracing method coupled with spherical sector analysis and dose depth curve to model radiation dose deposition on geometries described in the GDML format is used to estimate the Total Ionizing Dose (TID) deposited on a simplified 6U CubeSat geometry from protons. The CubeSat is exposed to a solar proton fluence, simulated using the Solar Accumulated and Peak Proton and Heavy Ion Radiation Environment (SAPPHIR). SSAM results are compared with those obtained from another dose calculation software utilizing the same methodology.**

The inter-comparison results demonstrate a good agreement between the two software and the accuracy and reliability of SSAM in capturing dose distribution patterns when compared to the reference software. Furthermore, an illustrative example showcases SSAM's application on a realistic 1U CubeSat geometry, highlighting its versatility in modelling radiation dose effects on complex space structures and in variable environments.

***Index Terms*—Total Ionized Dose, Ray-tracing, sector-shielding analysis, space weather forcast**

I. Introduction

THE space environment is populated by a wide variety of energetic particles, whether they originate from the sun, are trapped by planetary magnetic fields, or come from cosmic sources, they are capable of posing a threat to the integrity of spacecraft. Consequently, spacecraft design must take into account the various risks induced by these radiations, including electrostatic discharges resulting from the internal and surface charging, single events in computer memories, or the cumulative effect of total ionizing dose (TID), which damages electronic components [1].

To address all these risks, SpaceSuite offers software including SPIS-SC [2] and SPIS-IC [3] to simulate internal and surface charging processes, EDGE (ExtendeD GDML Editor) [4] to design geometries for internal and surface charging analysis or SEE-U [5], to perform single event effect (SEE) analysis. To simulate the TID, two types of methods are commonly used. On the one hand, Monte-Carlo methods, which provide a statistical result by modelling all interactions (secondary electron emission, Bremsstrahlung, ...) of a wide variety of primary particles. On the other, the sector shielding analysis method, is based on a geometric ray-tracing method to compute the equivalent shielding in each direction around one specific point. This last approach allows calculating the TID thanks to a precomputed dose depth curve.The dose depth curve is usually processed from Monte-Carlo simulations which contains any relevant interactions. SpaceSuite addresses both approaches respectively thanks to MoORa (Modelling Of Radiations), a user-friendly software modelling the charge and energy deposition with GRAS (Geant4 Radiation Analysis for Space) [6], a modular tool for space environment simulation based on the Monte-Carlo numerical kernel Geant4 [7], on the other hand to the Sector Shielding Analysis Module (SSAM), available as an EDGE module.

Several studies were carried out to perform inter-comparison of proton induced TID on spacecrafts from shielding analysis tools. Pourrouquet *et al.* [8] compared the dose deposition on simple spheres and 1D geometries submitted to electron and proton fluxes from AE8/AP8 [9] calculated with three Monte-Carlo codes. Finally, Jun *et al.* [10] realized a study comparing the dose deposition from MCNP, Geant4, NOVICE with adjoint Monte-Carlo and FASTRAD® with Forward and Adjoint Monte-Carlo and FASTRAD with ray tracing. In this last study, simple and realistic geometries were submitted to proton and electrons fluxes from Europa-Clipper.

After their conquest of low Earth orbit (LEO) and some forays into the medium and geostationary orbit (MEO and GEO) domains, in 2018 CubeSats reach the interplanetary orbit. This new mission destination for CubeSats poses increased space radiation threats to their material and payload. In this context, Sanders carried out a numerical study to investigate the proton radiation shielding capabilities of CubeSat bus structures under interplanetary environment exposure and find improved designs [11] using the FASTRAD simulation tool.

MoORa has already been the subject of serious validation and is used for scientific studies were already performed [3], [12]. In order to present SSAM and testified to its reliability, this software has been used to reproduce the Sanders' analysis and perform an inter-comparison of SSAM and the FASTRAD sector shielding analysis tools.

Next illustration cases are proposed on a realistic 1U CubeSat. First case reuses the proton environment computed for the validation study, to explore the influcence of the shielding thikness variation and detesselation on the dose deposition on the real CubeSat. The second case illustrate the feasibility of a dose rate daily forecast, by including SSAM in a simulation framework simulating the electron flux spectrum evolution along a geostationnary orbit thanks to the

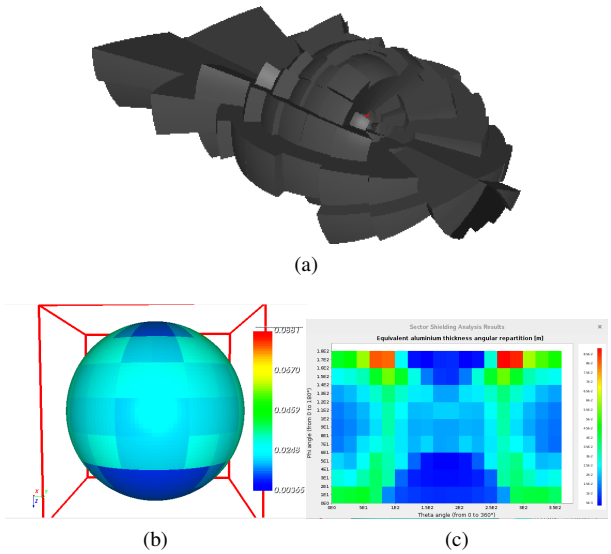

(a) (b) (c)

Fig. 1: Sector shielding analysis visualisation in SSAM: (a) sector view, (b) colourized spheres, (c) angular maps.

Fokker-Planck electron distribution function code VERB [13] (Versatile Electron Radiation Belt).

II. SSAM Presentation

The dose deposition analysis is performed with the Sector Shielding Analysis Module (SSAM), a module for the GDML (Geometry Description Markup Language) editor EDGE module. Through a simple and easy to use GUI, it allows performing shielding analyses and quick deposited dose computations at a given set of points defined through their coordinates and/or on GDML shapes. SSAM is perfectly adapted to quick radiation analysis, in a simple engineering approach or as preprocessing for more advanced modelling with MoOra.

It works by dividing the space around a point into a set number of sectors and following rays from this point up to the external boundary of the GDML environment. The material depth seen along the rays is calculated, which is used to calculate the maximum, minimum, and average shielding following each sector. SSAM provides numerous 3D representations of the evaluated shielding, like thickness for each sphere sector, colourized spheres and angular maps (cf. Figure 1). Finally, SSAM is able to calculate the dose deposited at a target point using a precomputed deposition function.

III. Simplified 6U-CubeSat TID analysis and inter-comparison with FASTRAD

A. Simplified CubeSat Geometry

To comply with the Sanders' study [11], the TID analysis is performed on a hollow parallelepiped box representing simplified CubeSat geometry. The reference for outer dimensions of the spacecraft structure are taken from the providers of CubeSat materials, ISIS. These outer dimensions are a length of 226.3 mm a width of 100.0 mm and a height of 340.5 mm. The inner part of the spacecraft is shielded with one or more layer of different material, meaning that the increasing of the shield thickness induce a decreasing of the free volume inside the spacecraft. As it can be seen on Table I, 10 different shields have been tested which can be grouped as follows:

TABLE I: Shielding configuration summary

Case	Shield layers structure Mat. Type + Thickness (mm)	Eq. Al thickness mm
1	Al1.0	1.0
2	Al2.0	2.0
3	Al3.0	3.0
4	Al5.0	5.0
5	Al0.5-PE0.5-Al0.5	1.174
6	Al0.5-PE1.0-Al0.5	1.348
7	Al1.0-PE1.0-Al1.0	2.348
8	Al0.5-Cu0.1-PE0.8-Cu0.1-Al0.5	1.943
9	Al1.0-Cu0.1-PE0.8-Cu0.1-Al1.0	2.943
10	Al1.0-Cu0.1-PE2.8-Cu0.1-Al1.0	3.639

- Cases 1 – 4 use pure aluminium shield,
- Cases 5 – 7 use a shield made with a polyethylene (PE) layer between two aluminium layers,
- Cases 8 – 10 use a shield made with a polyethylene (PE) layer between two copper layers, themselves cover with aluminium layers,

Knowing the symmetries of the box, the dose analysis of a single octant is representative of the whole geometry. For each shield, inside the spacecraft the TID is calculated at three points: at the centre of the spacecraft, halfway from the centre and one of a corner of the shield and at a corner.

B. Environment and dose deposition curve

The CubeSat with all its shield configurations is assumed to be located at 1 UA from the sun in the interplanetary environment and is submitted to a single proton fluence spectrum, deduced from the Solar Accumulated and Peak Proton and Heavy Ion Radiation Environment (SAPPHIRE) model [14]. This is a data model deduced from cleaned and post-processed *in-situ* measurements of the Solar Energetic Particle (SEP) environment. It notably includes maximum

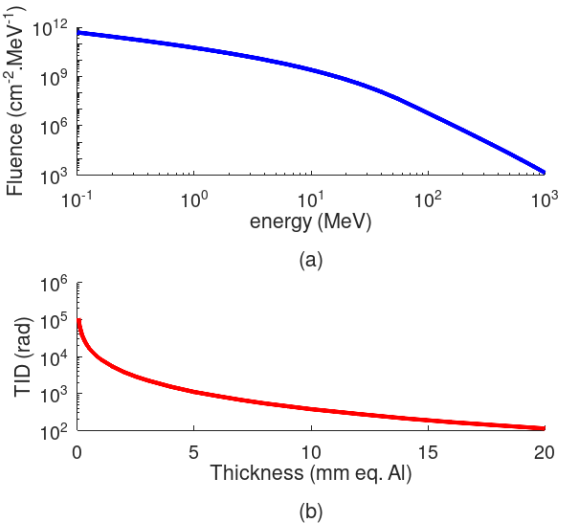

(a) (b)

Fig. 2: (a) Proton fluence differential spectrum, (b) TID deposed in pure Silicon under a spherical Aluminium shield with a given thickness.

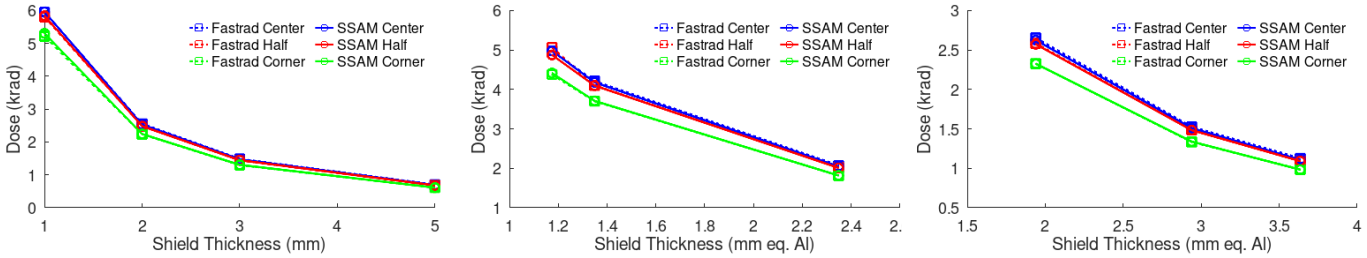

(a) (b) (c)

Fig. 3: TID deposition simulated with Fastrad and SSAM at each detection point according to the equivalent aluminium shield thickness for(a) Cases 1-4 with Shield in pure aluminium, (b) Cases 5-7 with a Al-PE-Al shield, (c) Case 8-10 with a Al-Cu-PE-Cu-Al shield.

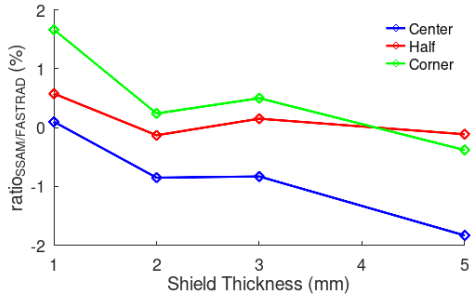

Fig. 4: TID ratio between SSAM and FASTRAD simulations at each detection point for pure aluminium shields.

event fluence spectra in terms of 1-in-x-year SPEs. In the frame of this study, SAPPHIR is used to provide the proton fluence differential displayed on Figure 2.a and corresponding to a 4-day exposition the 1-in-100-year has been selected.

In order to be used in SSAM, the proton fluence spectrum must be converted into a dose deposition function depending on the shielding thickness. This function is obtained from Shieldose2, the evolution of Shieldose [15]. It allows calculating the ionized dose deposition on a detector made with a chosen material and shielded with an aluminium layer. Shieldose2 support three types of geometric configuration. In the frame of this study, the configuration where the detector is included in a solid sphere isotropically irradiated is selected. The dose deposition curve obtained is presented in Figure 2.b and was calculated for a pure silicon detector.

C. Results

The TID is computed by SSAM at each detection point by tracing 10^6 rays and dividing the space into 1800 sectors. This number of sectors is obtained by an angular discretization of 60 in latitude and 30 in longitude.

The TID deposition simulated with SSAM and FASTRAD for all detection points are displayed for pure aluminium shield, for Al-PE-Al and Al-Cu-PE-Cu-Al configuration respectively on Figures 3.a 3.b and 3.c according to the aluminium equivalent shield thickness.

Whatever the used software, the detection point or the shield configuration, clearly visible is the sharp deposition thickness decrease with the shield depth. For both software, no significant difference in dose deposition can be observed between the central point and the point located halfway from the centre and the CubeSat corner and point out the fact that the radiation exposition is slightly lower at the corner. Indeed, the Figure 4 witnesses, for pure aluminium shield, of the very good agreement between both software result for the 3 detectors with an absolute relative difference staying under 2% in any case. The observed between-method differences remain acceptable.

IV. Application to a realistic 1U-CubeSat

A. Effect of the detessellation

Previous sections demonstrated that the SSAM plug-in for EDGE computes the same TID results as the commercial FASTRAD application for a 6U CubeSat. In this section, EDGE and SSAM are used to define the geometry of a realist 1U CubeSat and compute TID on several components inside.

In this case, 1U CubeSat geometry is defined in the industrial STEP-AP 203/214 file format, which is usually used for engineering models. This file has been used with the courtesy of Flavino Crespi and is available on the GRAB CAD website. As illustrated in Figure 5, the CubeSat has two solar panels, a boundary structure considered in aluminium and a circuit board with 421 components on it and considered silicon material. The DeCADe plug-in for EDGE imports all shapes from STEP AP file by meshing them on a surface. Surface mesh shapes are called tessellated shapes.

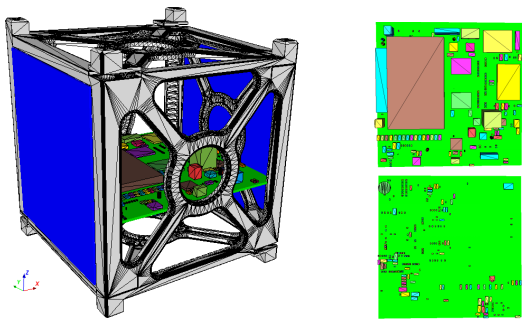

(a) (b)

Fig. 5: GDML view in edge of (a) the tessellated 1U CubeSat geometry (b) The printed circuit board included inside the CubeSat. (Courtesy of Flaviano Crespi)

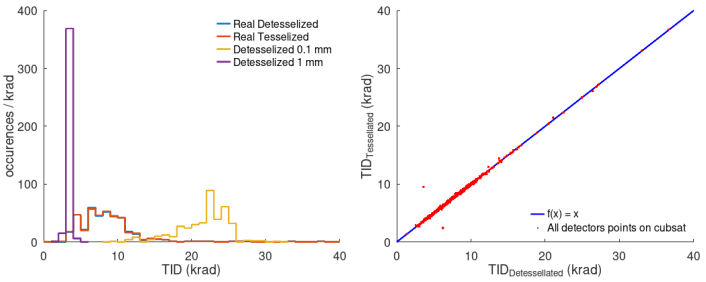

(a) (b)

Fig. 6: (a) Histogram of dose deposited on all detection points. (b) Dose deposition comparison for tessellated and detessellated geometries with realistic shield

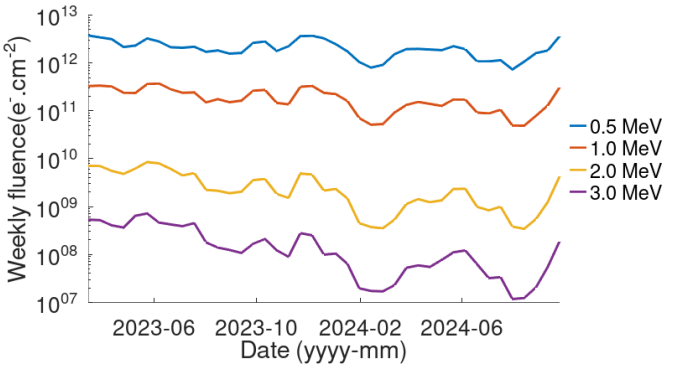

Fig. 7: Integrated electron flux spectrum evolution along the studied period.

The TID of 390 components have been computed by SSAM with different configurations on the geometry:

- Case 1: The external structure of the CubeSat comes from the STEP-AP file. The components inside the CubeSat are **tessellated**.
- Case 2: The external structure of the CubeSat comes from the STEP-AP file. The components inside the CubeSat are **detessellated**.
- Case 3: The external structure of the CubeSat is modelled by a hollow box with 0.1 mm aluminium thickness. The components inside the CubeSat are **detessellated**.
- Case 4: The external structure of the CubeSat is modelled by a hollow box with 1 mm aluminium thickness. The components inside the CubeSat are **detessellated**.

Using tessellated shapes for dose calculation modelled with a Monte Carlo method, such as Geant4, can increase CPU calculation time and change the accuracy of the results [16]. To solve this problem, DeCADe is used for detessellation, which means to build a GDML atomic shape (box, cylinder, cone, ellipsoid, etc.) from a tessellated shape. Thanks to EDGE, which allows you to calculate the mass of each shape of a CAD model, the thickness of the shielding of case 4 is set to 1 mm which makes its mass the same as cases 1 and 2 to evaluate the impact of the anisotropy of shielding on the dose.

Figure 6.a displays the distributed differential function of the TID calculated for each configuration. Case 3 has the highest TID value because its shielding thickness is the thinnest of all cases. The min and max TID values are 9 krad and 31 krad respectively. In this case, the TID value strongly depends on the position in the CubeSat, as explained in the previous sections. The TID values calculated for case 1 are compared to case 2. The values are the same, as shown in Figure 6.b and 6.a. This validates the detasseling of 421 shapes having a total of 6382 triangles. SSAM allows us to calculate the minimum and maximum shielding thickness seen by a position. For cases 1 and 2, the shielding seen by a position varies from 0 to 50 mm depending on the direction. The TID values of case 4 are lower than those of cases 1 and 2 while the mass of their shielding is the same. This shows that for this study, where the TID is calculated for protons, isotropic shielding gives a lower TID than with strongly anisotropic shielding. Other geometric configurations need to be investigated to be able to find an optimized constant mass design to find the lowest TID.

B. Deposited dose estimation in a time dependent GEO environment

The last study consists in the realisation of an estimation of the evolution of the dose rate and the total deposited ionizing dose evolution on the PCB card of the Cubesat presented on Figure 5 orbiting the earth in a geostationary orbit. For aluminium shielding thickness up to $5\,mm$, the TID is for the most part induced by primary electrons [17].

Electron fluxes along a $137°W$ geostationary orbit from `2023-02-28` to `2024-09-18` are derived using the PAGER framework day + 1 forecast. This forecast is primarily based on the radiation belt electron distribution function modeled with VERB [13], [18], where fluxes are computed in accordance with the T89 geomagnetic field model [19]. These fluxes are subsequently employed to calculate weekly fluences, enabling an in-depth analysis of radiation exposure over the specified time period. The integrated fluxes evolution fir different energy threshold is displayed on Figure 7.

From the calculated deposition curves, which are obtained using Shieldose2 with electron fluence spectra of the figure 7 as input, the SSAM tool determines the mean, maximum, and minimum doses deposited by electrons on each sector of a spherical detector. This process is performed dynamically for each component of the electronic card, following a straightforward selection of all relevant elements. This efficient methodology ensures accurate dose evaluations across all card components while maintaining ease of implementation. In this case, dose deposition has been calculated using mean shield thickness for each sector of sphere.

A histogram of the accumulated dose over the entire period is displayed on Figure 8.a. It highlights significant variability depending on the specific electronic element analyzed. Maximum dose reaches 42 krads, but most of the coponents received a TID $<$ 23 krads. The dose deposition and dose rate trends over time are displayed on Figure 8.b. Dose rate evolution closely mirrors the temporal variations of the integrated electron flux within the geostationary environment. This observation underscores the strong dependence of radiation

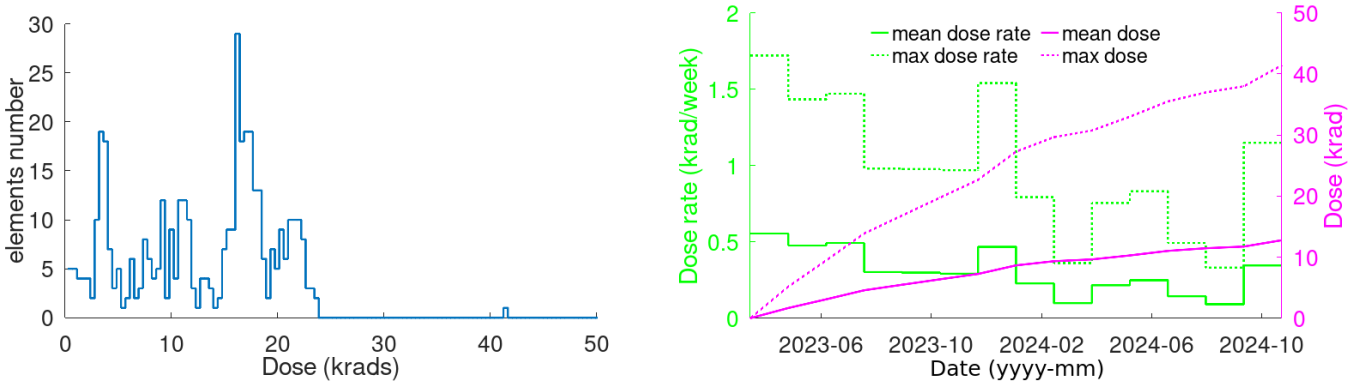

(a) (b)

Fig. 8: (a) histogram of the total dose deposited over the period studied on all of the electronic components in the spacecraft. (b) evolution of the mean and maximal dose rate and TID deposited on spacecraft components.

exposure on the dynamics of the space weather environment, emphasizing the need for robust modeling and forecasting to predict and mitigate its impact on satellite components.

V. Conclusion

SSAM is an efficient tool to perform dose deposition estimation from sector shielding analysis. The SSAM addition in EDGE relies on the GDML geometry used in Geant4 (Monte-Carlo) simulations, making it a key component of the SpaceSuite software, which aims to address all environmental risk analysis on spacecraft. Its user-friendly graphic interface allows you to easily select the location of numerous the dose measurement points and perform quick analyses, while its synergy with DeCADe makes it possible to deal with complex and realistic geometries, making EDGE a valid tool for spacecraft or payload design applications

The comparison of SSAM simulations with another sector-shielding-analysis tool on a simple 6U CubeSat under interplanetary proton fluence gives very similar result, whatever the shield structure and detector location. This demonstrates its reliability for calculating the dose deposited by protons.

The estimation of the dose deposited on a cubesat in geostationary orbit using data from PAGER shows the feasibility of using SSAM downstream of a space weather forecast model, paving the way for its use in the context of an automated framework for predicting the effect of the space environment on realistic satellite geometries

Acknowledgment

Thanks to Fabio for allowing us to use the geometry of the 1U cubesat. The original fill is available at: https://grabcad.com/library/cubesat-module-1/details?folder_id=1159696

References

[1] Y. Lu, Q. Shao, H. Yue, and F. Yang, "A Review of the Space Environment Effects on Spacecraft in Different Orbits," *IEEE Access*, vol. 7, pp. 93 473–93 488, 2019. DOI: 10.1109/ACCESS.2019.2927811.

[2] B. Thiebault, B. Jeanty-Ruard, P. Souquet, *et al.*, "SPIS 5.1: An Innovative Approach for Spacecraft Plasma Modeling," *IEEE Trans. Plasma Sci.*, vol. 43, no. 9, pp. 2782–2788, 2015. DOI: 10.1109/TPS.2015.2425300.

[3] B. Jeanty-Ruard, P. Sarrailh, D. Payan, *et al.*, "Internal Charging Analysis of a Space Instrument in PEO with a Dedicated Modeling Chain," *IEEE Trans. Plasma Sci.*, vol. 47, no. 8, pp. 3699–3709, 2019. DOI: 10.1109/TPS.2019.2911408.

[4] A. Trouche, B. Jeanty-Ruard, N. Chabalier, and J. Forest, "EDGE, ExtendeD GDML Editor: A new GMDL CAD tool for GEANT4 based analysis and interoperability bridge for high-energy particle modelling tools," in *ENSAR2 workshop: GEANT4 in nuclear physics*, Madrid, Spain, 2019.

[5] L. Artola, B. Jeanty-Ruard, J. Forest, and G. Hubert, "Soft Error Simulation of Near-Threshold SRAM Design for Nanosatellite Applications," *Electronics*, vol. 12, no. 18, p. 3968, 2023. DOI: 10.3390/electronics12183968.

[6] G. Santin, V. Ivanchenko, H. Evans, P. Nieminen, and E. Daly, "GRAS: A General-Purpose 3-D Modular Simulation Tool for Space Environment Effects Analysis," *IEEE Trans. Nucl. Sci.*, vol. 52, no. 6, pp. 2294–2299, 2005. DOI: 10.1109/TNS.2005.860749.

[7] J. Allison, K. Amako, J. Apostolakis, *et al.*, "Geant4 Developments and Applications," *IEEE Trans. Nucl. Sci.*, vol. 53, no. 1, pp. 270–278, 2006. DOI: 10.1109/TNS.2006.869826.

[8] P. Pourrouquet, A. Varotsou, L. Sarie, *et al.*, "Comparative Study Between Monte-Carlo Tools for Space Applications," in *16th European Conference on Radiation and Its Effects on Components and Systems (RADECS)*, 2016. DOI: 10.1109/radecs.2016.8093121.

[9] E. J. Daly, J. Lemaire, D. Heynderickx, and D. J. Rodgers, "Problems with Models of the Radiation Belts," *IEEE Trans. Nucl. Sci.*, vol. 43, no. 2, pp. 403–415, 1996. DOI: 10.1109/23.490889.

[10] B. Jun, B. X. Zhu, L. M. Martinez-Sierra, and I. Jun, "Intercomparison of Ionizing Doses From Space Shielding Analyses Using MCNP, Geant4, FASTRAD, and NOVICE," *IEEE Trans. Nucl. Sci.*, vol. 67, no. 7, pp. 1629–1636, 2020. DOI: 10.1109/TNS.2020.2979657.

[11] T. Sanders, "Spacecraft Radiation Shielding Study of a 6U-CubeSat in Interplanetary Orbit," M.S. thesis, Delft University of Technology, 2018.

[12] B. Tezenas du Montcel, A. Trouche, I. Michaelis, B. Jeanty-Ruard, M. Wutzig, J. Forest, and Y. Y. Shprits, "Presentation and validation of the internal charging risk forecast in the PAGER framework," *Adv. Space Res.*, vol. 72, no. 9, pp. 3666–3676, 2023. DOI: 10.1016/j.asr.2023.07.047.

[13] D. A. Subbotin and Y. Y. Shprits, "Three-dimensional modeling of the radiation belts using the Versatile Electron Radiation Belt (VERB) code," *Space Weather*, vol. 7, no. S10001, 2009. DOI: 10.1029/2008SW000452.

[14] P. Jiggens, D. Heynderickx, I. Sandberg, P. Truscott, O. Raukunen, and R. Vainio, "Updated Model of the Solar Energetic Proton Environment in Space," *J. Space Weather Space Clim.*, vol. 8, no. A31, 2018. DOI: 10.1051/swsc/2018010.

[15] S. M. Seltzer, "Conversion of Depth-Dose Distributions from Slab to Spherical Geometries for Space-Shielding Applications," *IEEE Trans. Nucl. Sci.*, vol. 33, no. 6, pp. 1292–1297, 1986. DOI: 10.1109/TNS.1986.4334595.

[16] J. Forest, B. Jeanty-Ruard, A. Trouche, *et al.*, "Examples of applications cases of geant4 in space environment effects analysis with the spacesuite tools and feedbacks," in *14th Geant4 Space Users Workshop*, Korinthia, Greece, 2019.

[17] J. Solin, "The geo total ionizing dose," *IEEE Trans. Nucl. Sci.*, vol. 45, no. 6, pp. 2964–2971, 1998. DOI: 10.1109/23.736553.

[18] D. A. Subbotin and Y. Y. Shprits, "Three-dimensional radiation belt simulations in terms of adiabatic invariants using a single numerical grid," *J. Geophys. Res.*, vol. 117, no. A05205, 2012. DOI: 10.1029/2011JA017467.

[19] N. Tsyganenko, "A Magnetospheric Magnetic Field Model with a Warped Tail Current Sheet," *Planet. Space Sci.*, vol. 37, no. 1, pp. 5–20, 1989. DOI: 10.1016/0032-0633(89)90066-4.